of the RC column. In addition, the difference of maximum moment capacity is about 10%. The displacement ductility of the precast columns is about 2.0-2.3 times the displacement ductility of the RC column. The energy dissipation of the precast columns is about 1.6-2.0 times the energy dissipation of the RC column. The failure of both RC and precast columns is due to the buckling of the bar and splice under compression.

5. A sensitivity study is conducted by increasing the volumetric of lateral reinforcement from 0.77% to 1.78%. It is found that the curvature ductility of the RC column is 1.10 times the curvature ductility of the precast columns at different coupler gap lengths. However, the maximum moment capacity is different from the precast columns by 1.4-3.5%. The tension rupture of couplers can limit the ductility in columns.

6.2 Recommendations

The following future works should be carried out to be able to conduct a more thorough investigation of the mechanical splice's behavior.

1. Other types of steel grade for both reinforcing bar and coupler should be subjected to further tests.

2. Different types of columns and tie configurations should be taken into consideration so as to gain thorough understanding of the corresponding energy dissipation of the precast columns with mechanical splices and RC columns.

REFERENCES

American Concrete Institute Committee 318 (2002). Building Code Requirements for Structural Concrete (ACI318-05) and Commentary (ACI 318R-05).

Ancon Building Products (2005). Reinforcing Bar Couplers for the Construction Industry.

Billington, S.L., Barnes, R.W. and Breen, J.E. (2001). Alternate Substructure Systems for Standard Highway Bridges, ASCE Journal of Bridge Engineering, 6, 2:87-94.

Billington, S.L. and Yoon, J.K. (2004). Cyclic Response of Unboned Post-Tensioned Precast Column with Ductile Fiber-Reinforced Concrete, American Society of Civil Engineers, Journal of Bridge Engineering, 9, 4:353-363.

California Department of Transportation (2006). Prequalified List of Couplers on Reinforcing Steel, Structural Materials Testing Branch, Office of Structural Materials.

California Test 670 (1999). Method of Tests for Steel Reinforcing Bar Butt Splices, Department of Transportation, State of California, Business, Transportation and Housing Agency.

Cosenza, E. and Prota, A. (2006). Experimental Behavior and Numerical Modeling of Smooth Steel Bars under Compression, Journal of Earthquake Engineering, Imperial College Press, 10, 3:313-329.

Dextra Group and Distributors (2005). Product Datasheet Bartec Splice System.

Dhakal, R.P. and Maekawa, K. (2002). Modeling of Postyield Buckling of Reinforcement, Journal of Structural Engineering, 128, 9:1139-1147.

Dhakal, R.P. and Maekawa, K. (2002). Path-dependent Cyclic Stress-strain Relationship of Reinforcing Bar including Buckling, Engineering Structures, 24: 1383-1396.

Dhakal, R.P. and Maekawa, K. (2002). Reinforcement Stability and Fracture of Cover Concrete in Reinforced Concrete Members, Journal of Structural Engineering, 128, 10:1253-1262.

Einea, A., Yamane, T. and Tadros, M.K. (1995). Grouted-filled Pile Splices for Precast Concrete Construction, Precast / Prestressed Concrete Institute Journal, 40, 1:82-93.

Englekirk, R.E. (1982). Overview of ATC Seminar on Design of Prefabricated Concrete Buildings for Earthquake Loads, Precast / Prestressed Concrete Institute Journal, 80-97.

ERICO International Corporation (2005). Why a Mechanical Splice is Best in Reinforced Concrete.

ERICO International Corporation (2006). CADWELD Rebar Metal Filled Mechanical Splices.

Fouad, H.F., Rizk, T., Stafforf, E. and Hamby, D. (2006). A Prefabricated Precast Concrete Bridge System for the State of Alabama, University Transportation Center for Alabama, UTCA Report 05215.

Hieber, D.G., Wacker, J.M., Eberhard, M.O. and Stanton, J.F. (2005). Precast Concrete Pier Systems for Rapid Construction of Bridges in Seismic Regions, Final Research Report, Department of Civil and Environmental Engineering, University of Washington.

Hoshikuma, J., Kawashima, K., Nagaya, K. and Taylor, A.W. (1997). Stress-strain Model for Confined Reinforced Concrete in Bridge Piers, Journal of Structural Engineering, 624-633.

Kent, D.C. and Park, R. (1971). Flexural Members with Confined Concrete, Journal of Structural Engineering, American Society of Civil Engineers, 97, 7:1969-1990.

Masumoto, E.E., Kreger, M.E., Waggoner, M.C. and Sumen, G. (2002). Grouted Connection Tests in Development of Precast Bent Cap Systems, Transportation Research Record 1814, Transportation Research Board, Washington D.C., 55-64.

Monti, G. and Nuti, C. (1992). Nonlinear Cyclic Behavior of Reinforcing Bars Including Buckling, Journal of Structural Engineering, 118, 12:3268-3284.

Murat, S. and Razvi, S.R. (1992). Strength and Ductility of Confined Concrete, American Society of Civil Engineers, Journal of Bridge Engineering, 118, 6:1590-1607.

Nadim I., Wehbe, M., Saiid, S., and Sanders, D.H. (1999). Seismic Performance of Rectangular Bridge Columns with Moderate Confinement, American Concrete Institute Structural Journal, 96, 2: 248-258.

NBM Splice-Sleeve Systems, Splice Sleeve North America, Inc.

Park, R. and Priestly, N. (1982). Ductility of Square-Confined Concrete Columns, American Society of Civil Engineers, Journal of the Structural Division, 108, No.ST4: 929-951.

Park, R. and Priestly, N. (1987). Strength and Ductility of Concrete Bridge Columns under Seismic Loading, American Concrete Institute, Structural Journal.

Priestly, N. , Seible, F. and Calvi. (1996). Seismic Design and Retrofit of Bridges. USA: University of California, SanDiego. Italy: University of Pava

Rodriguez, M.E., Botero, J.C. and Villa, J. (1998). Cyclic Stress-strain Behavior of Reinforcing Steel Including Effect of Buckling, Journal of Structural Engineering, 125, 6:605-612.

Seible, F. and Hose, Y.D. (2000). Performance Evaluation Database for Concrete Bridge Components, Sub-assemblages and Systems under Simulated Seismic Loads, PEER Program, Department of Structural Engineering.

Sheikh, S.A. and Toklucu, M.T. (1993). Reinforced Concrete Columns Confined by Circular Spirals and Hoops, American Concrete Institute, Structural Journal, 90, 5: 542-553.

Sheikh, S.A. and Uzumeri, S.M. (1980). Strength and Ductility of Tied Concrete Columns, American Society of Civil Engineers, Journal of the Structural Division, 106, No.ST5:1079-1102.

Soudki, A, Rizkalla, H. and LeBlance. (1995). Horizontal Connections for Precast Concreted Shear Walls Subjected to Cyclic Deformations Part 1: Mild Steel Connections, Precast / Prestressed Concrete Institute Journal, 40, 3:78-96.

Standard Test Methods for Tension Testing of Metallic Materials (Metric), ASTM International, E 8M-04, 1-23.

Standard Specifications for Highway Bridges 17th Edition (2002). American Association of State Highway and Transportation Officials (AASHTO), ISBN: 156051-171-0.

Steel for Reinforcement of Concrete-Mechanical Splices for Bars, Part 1: Requirements, Draft International Standard, ISO/DIS 15835-1.

Steel for Reinforcement of Concrete-Mechanical Splices for Bars, Part 2: Test Methods, Draft International Standard, ISO/DIS 15835-2.

The Standard Drawing of Rural Highway, Department of Thailand.

Uniform Building Code, (1997). Structural Engineering Design Provisions, 2.

Wiss, Tanney, Elstner Associates, Inc. (2004). CALTRANS CT670 Tests on Bartec Reinforcing Bar Mechanical Splices, Final Report, WJE No.2004.3254.A, Dextra America Inc. and Dextra Manufacturing Co., Ltd.

APPENDIX

APPENDIX A

Table A.1 Control bar specimen under compression

Position (mm)	Load (KN)	Description	State	Deformed shape
0.00	0.00	initial	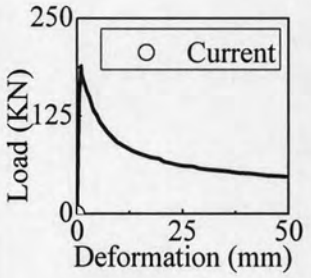	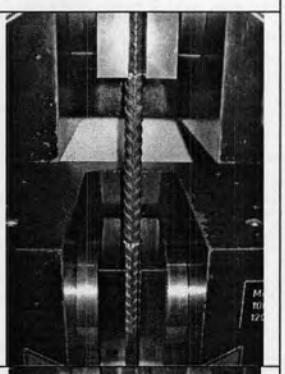
0.98	188.42	Start buckling	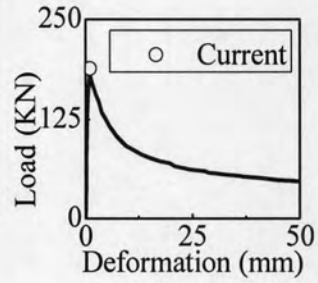	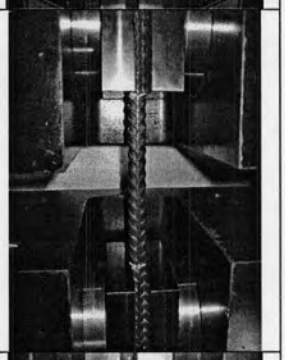
7.34	103.10	Non-linear softening	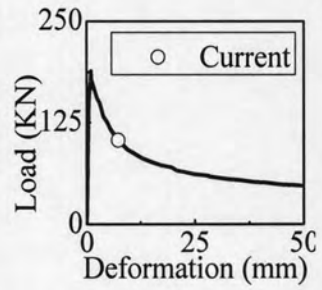	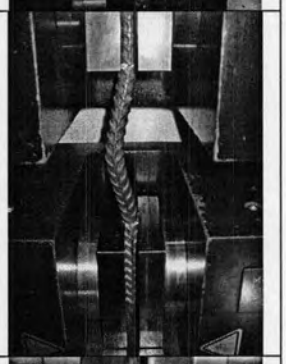
9.34	98.02	Non-linear softening	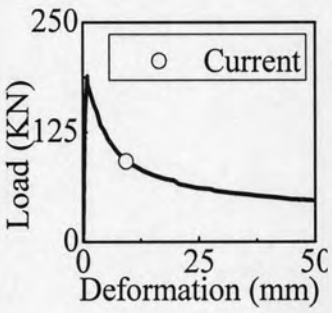	

15.14	76.0	Non-linear softening	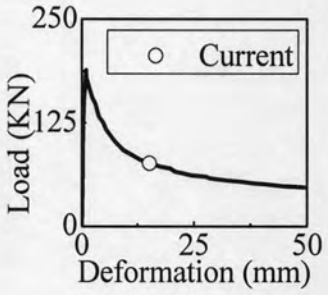	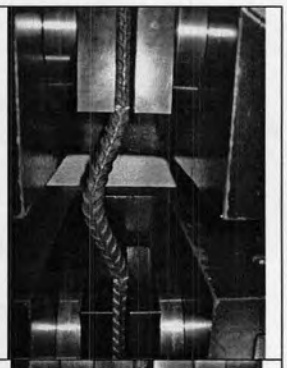
19.64	70.4	Non-linear softening	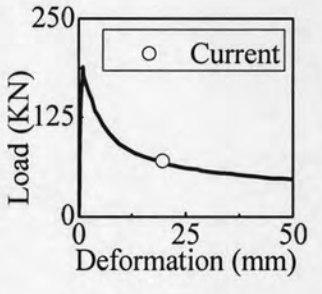	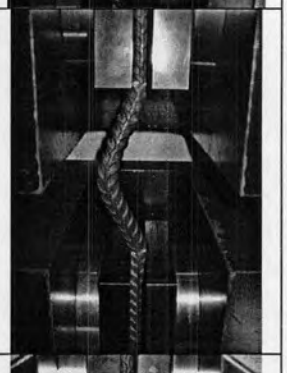
27.78	59.70	Non-linear softening	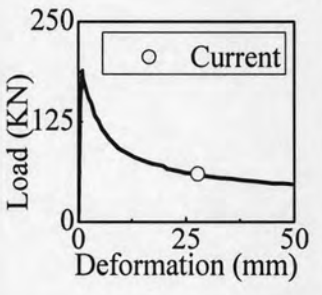	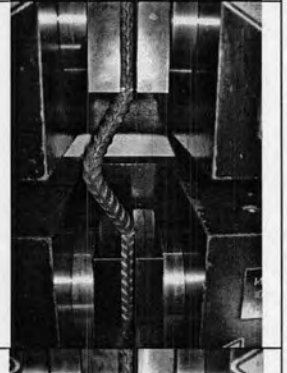
30.86	56.50	Non-linear softening	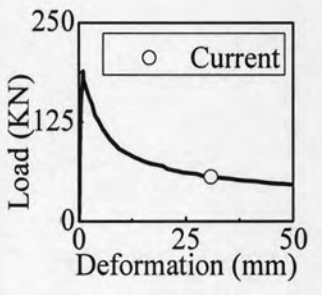	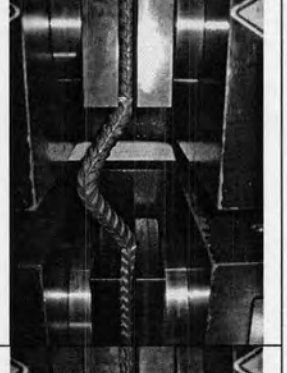
36.00	53.90	Non-linear softening	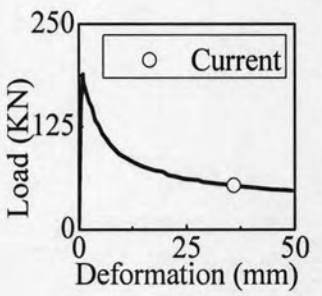	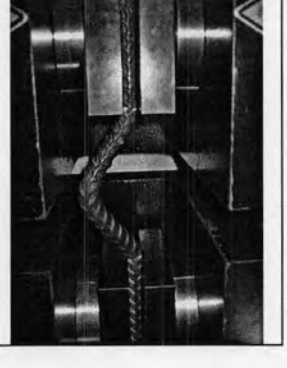

40.64	50.90	Non-linear softening	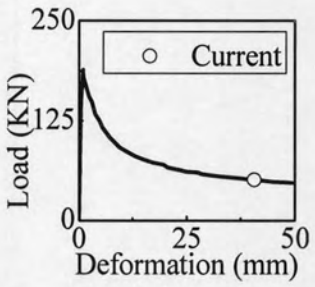	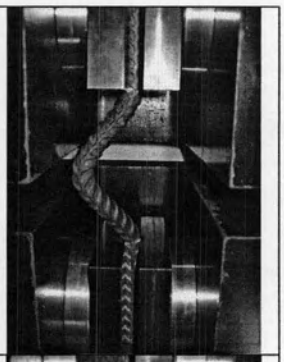
45.10	48.20	Non-linear softening	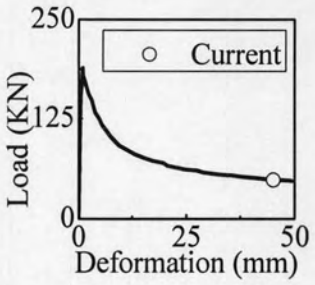	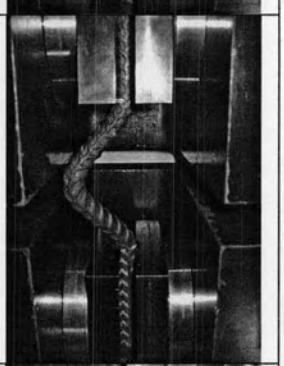
49.34	47.30	End	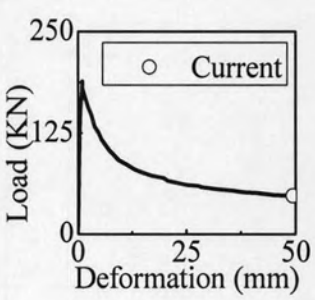	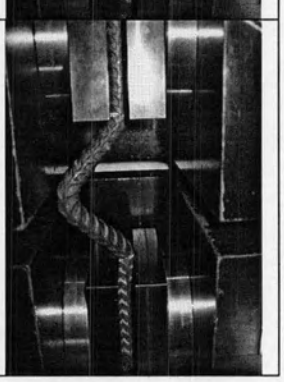

Table A.2 Specimen T4.0-G30 under compression

Position (mm)	Load (KN)	Description	State	Deformed shape
0.00	0.00	Initial	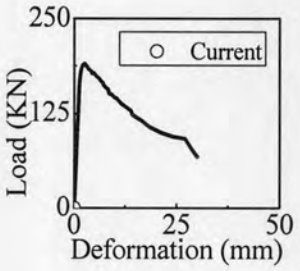	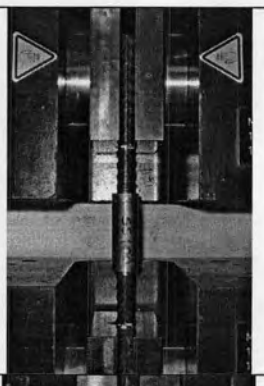
2.12	188.31	Start buckling	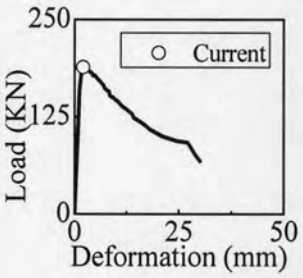	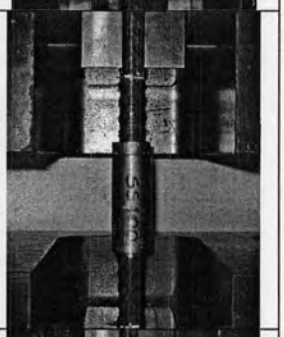
3.10	188.80	Non-linear softening	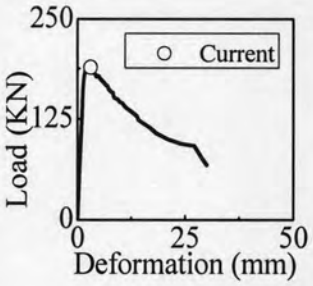	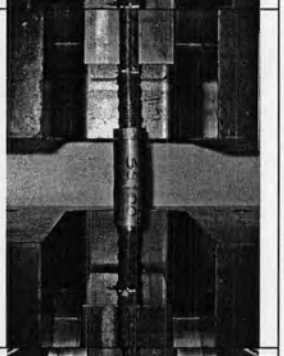
5.0	176.80	Non-linear softening	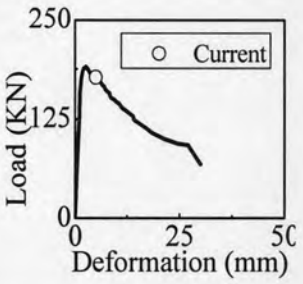	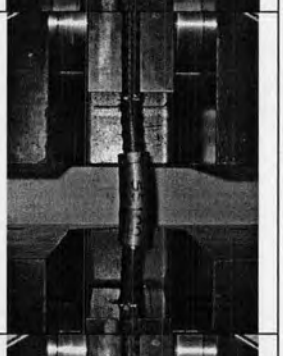
10.56	144.0	Non-linear softening	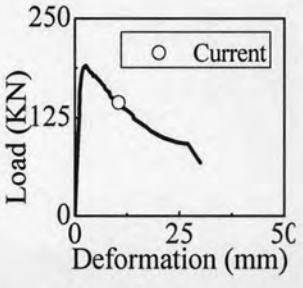	

15.46	119.0	Non-linear softening	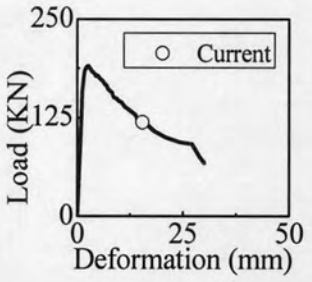	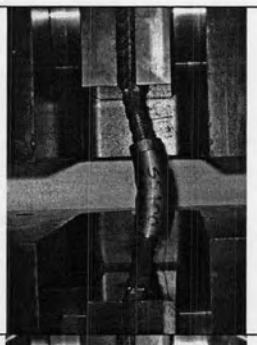
21.14	99.60	Non-linear softening	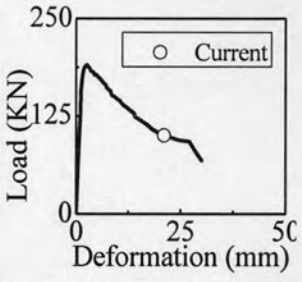	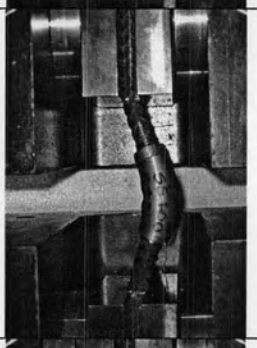
27.12	91.58	Non-linear softening	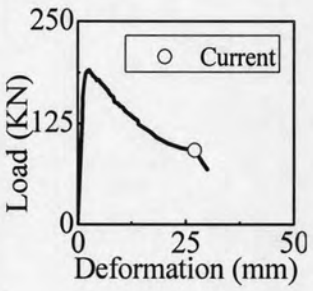	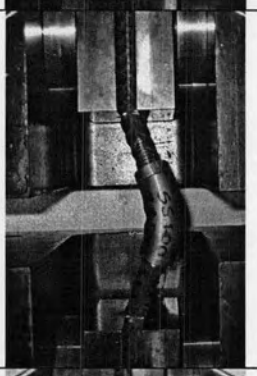
30.06	67.90	End	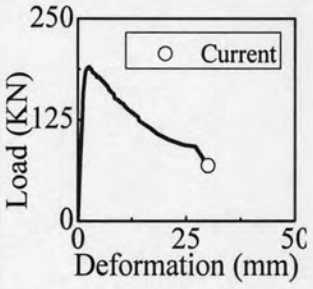	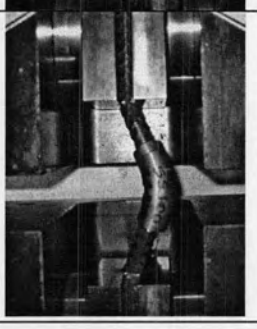

Table A.3 Specimen T4.0-G42 under compression

Position (mm)	Load (KN)	Description	State	Deformed shape
0.00	0.00	Initial	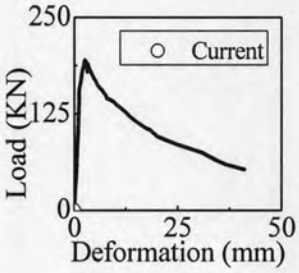	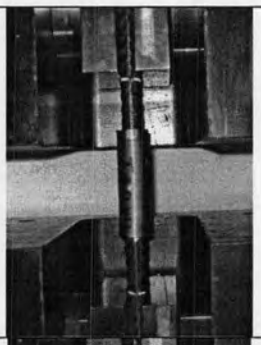
1.22	155.89	yielding	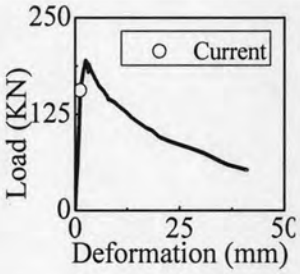	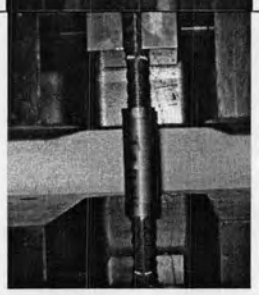
5.50	163.00	Non-linear softening	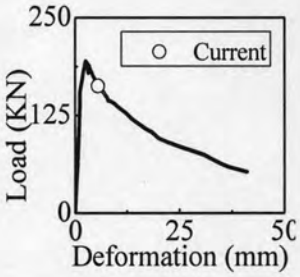	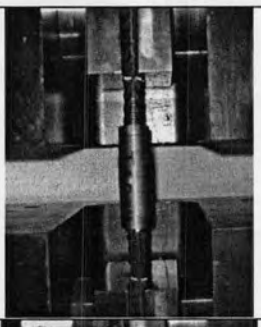
10.38	136.20	Non-linear softening	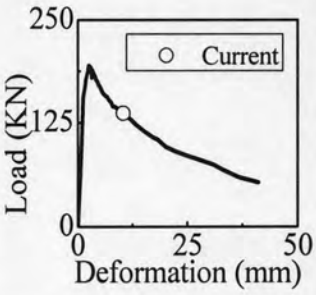	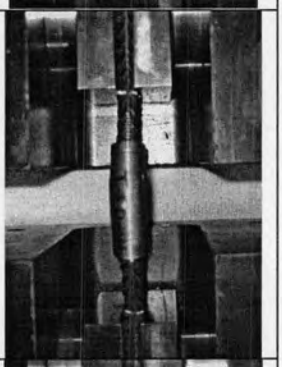
15.04	114.90	Non-linear softening	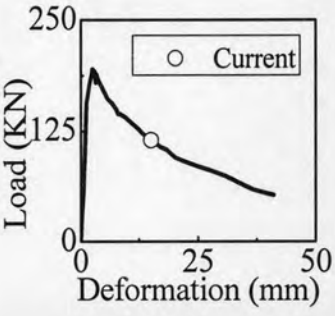	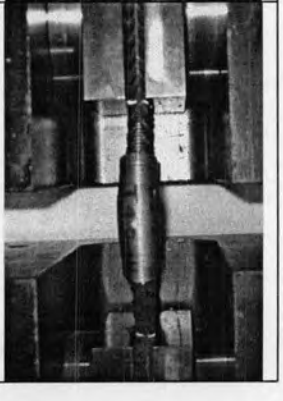

20.16	95.50	Non-linear softening	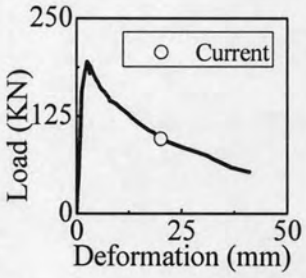	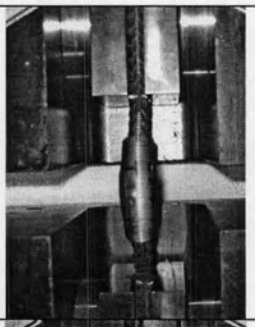
25.0	85.10	Non-linear softening	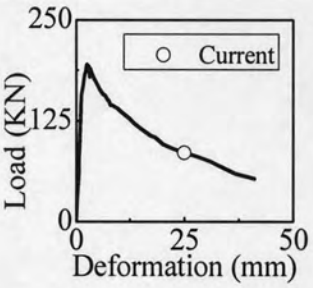	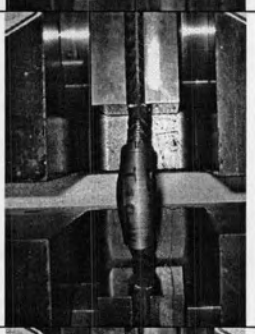
30.98	74.10	Non-linear softening	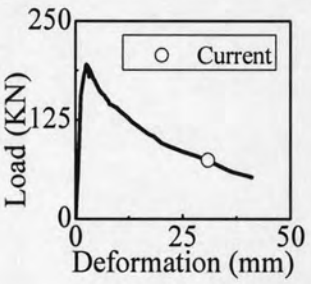	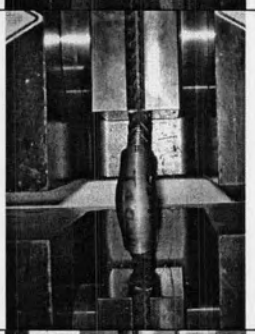
41.08	52.80	End	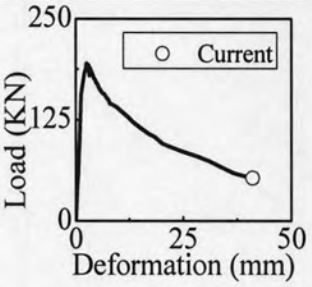	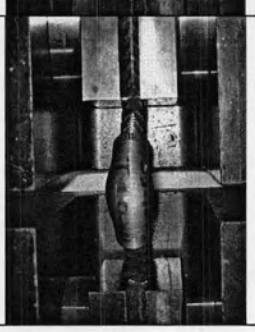

Table A.4 Specimen T4.0-G54 under compression

Position (mm)	Load (KN)	Description	State	Deformed shape
0.00	0.00	Initial	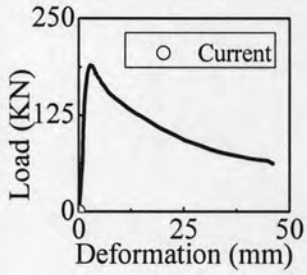	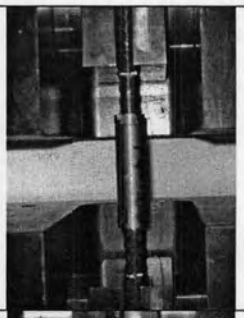
5.28	167.60	Non-linear softening	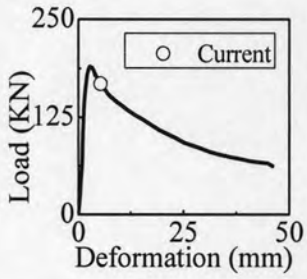	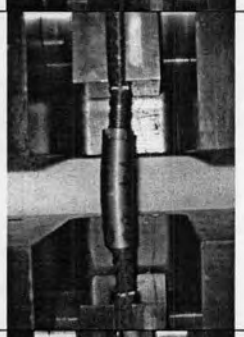
10.74	138.20	Non-linear softening	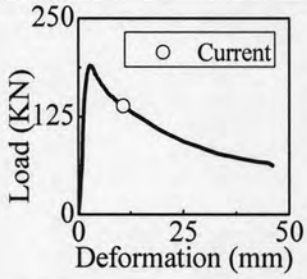	
15.10	122.70	Non-linear softening	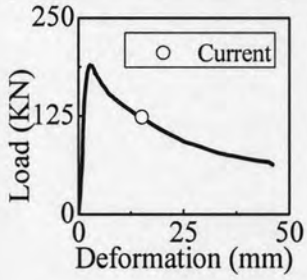	
21.56	102.50	Non-linear softening	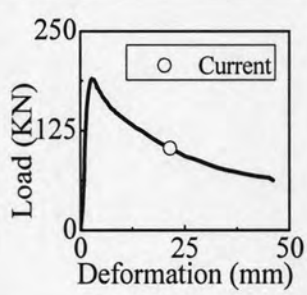	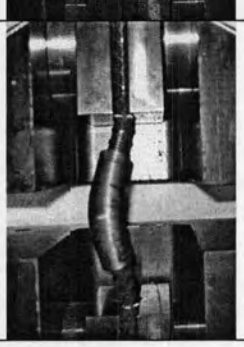

30.98	81.20	Non-linear softening	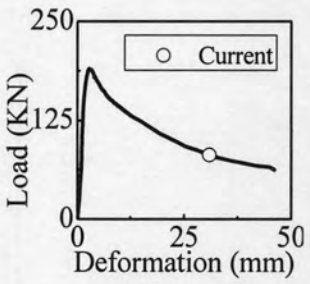	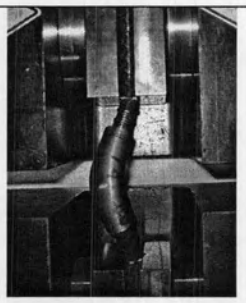
40.76	68.63	Non-linear softening	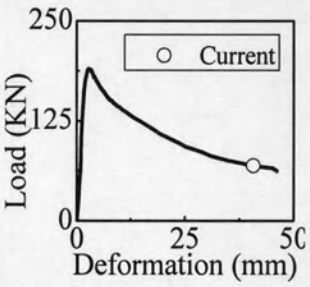	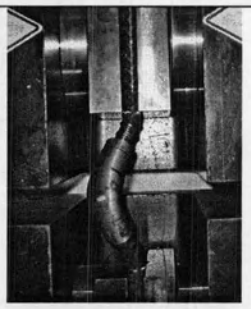
46.10	62.10	End	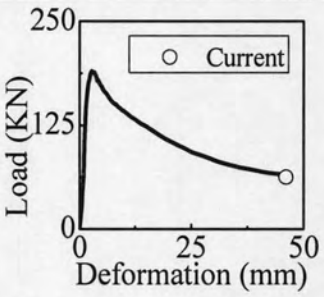	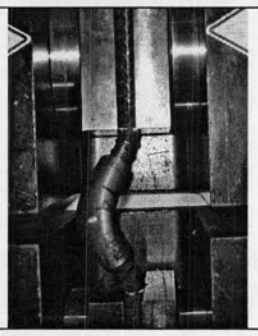

Table A.5 Specimen T4.0-G102 under compression

Position	Load	Description	State	Deformed shape
(mm)	(KN)			
0.00	0.00	Initial	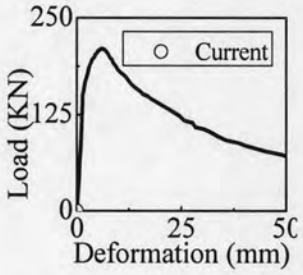	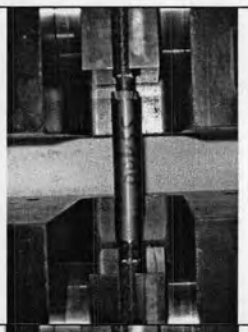
5.34	208.09	Non-linear softening	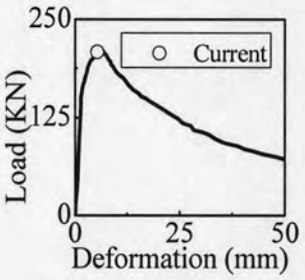	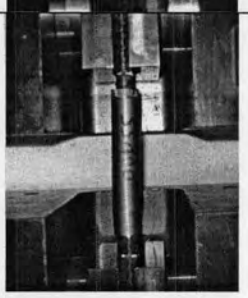
10.42	180.00	Non-linear softening	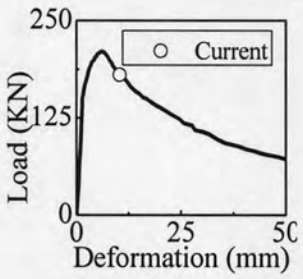	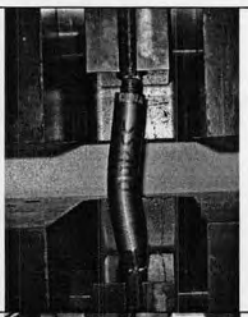
20.72	136.40	Non-linear softening	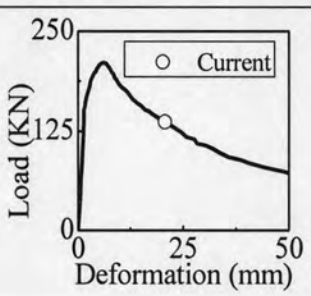	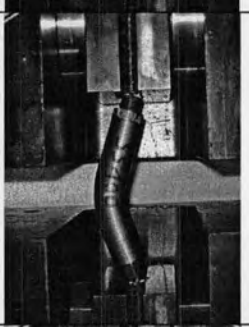
25.74	117.40	Non-linear softening	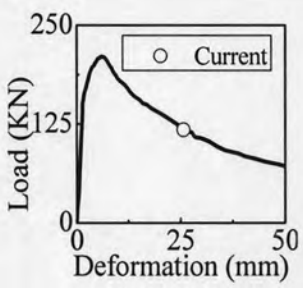	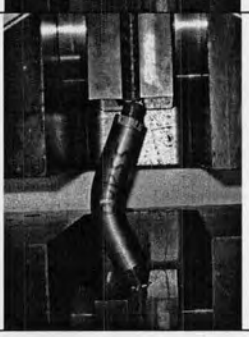

35.68	92.10	Non-linear softening	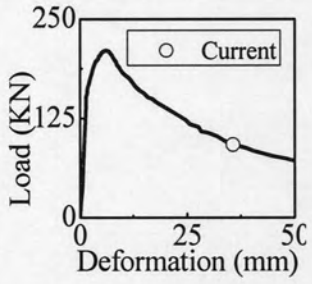	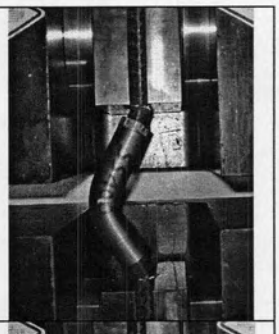
40.52	84.30	Non-linear softening	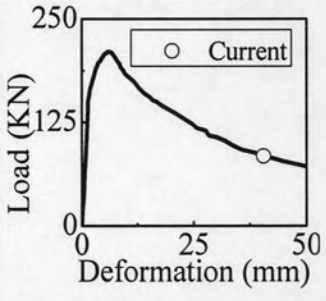	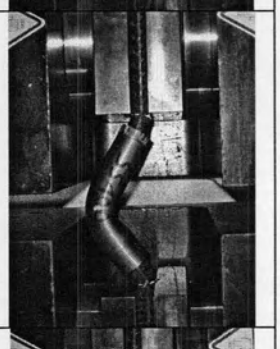
49.82	72.0	End	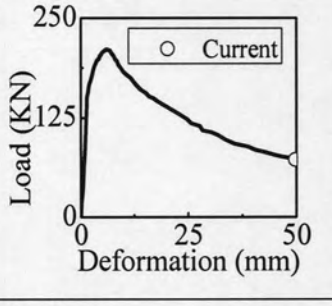	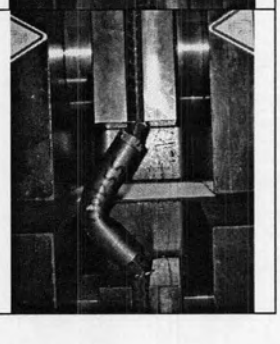

APPENDIX B

Table B.1 Control bar specimen under cyclic loading

Stroke	Deformation		Load		Energy	Cycle	State	Deformed shapes	
	$-\delta_{max}$	$+\delta_{max}$	$-P_{max}$	$+P_{max}$		No		Push down	Pull up
(mm)	(mm)	(mm)	(KN)	(KN)	(N.m)				
$\pm 0\delta_{cy}$	0.00	0.00	0.00	0.00	0.00	0		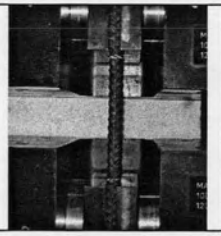	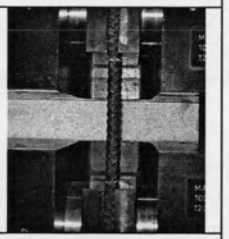
$\pm 6\delta_{cy}$	-2.62	2.02	-157.4	175.2	695.15	1	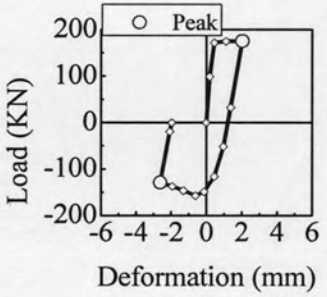	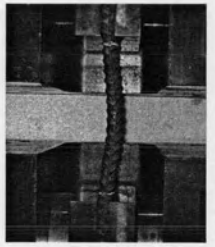	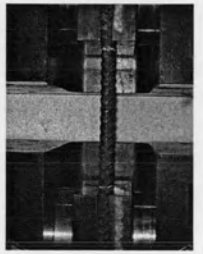

$\pm 18\,\delta_{cy}$	-11.5	7.22	-93.3	183.3	2316.42	5	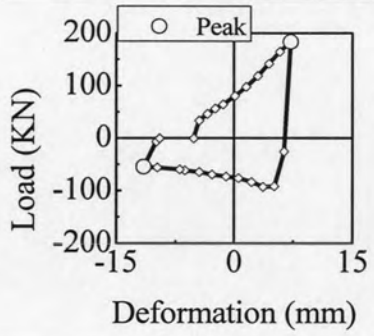	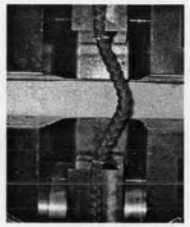	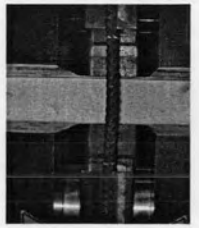
$\pm 18\,\delta_{cy}$	-12.74	7.28	-68.2	141.0	2104.9	6	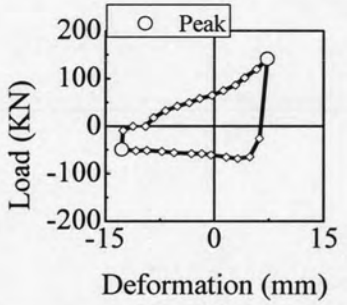	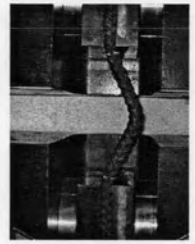	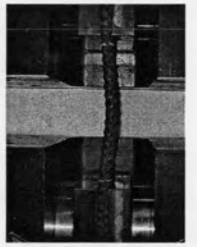
$\pm 24\,\delta_{cy}$	-16.54	10.08	-70.9	157.8	2439.41	7	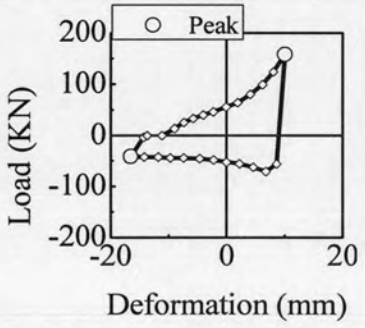		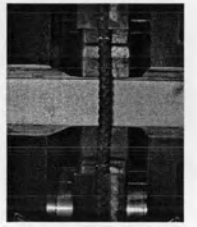

$\pm 24\delta_{cy}$	-13.67	8.72	0	72.07	855.41	8	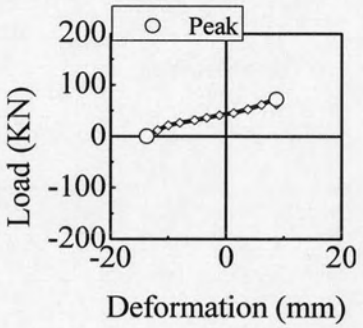	End	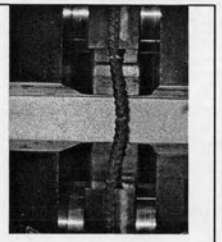

Table B.2 Specimen T4.0-G30 under cyclic loading

Stroke	Deformation		Load		Energy	Cycle	State	Deformed shapes	
	$-\delta_{max}$	$+\delta_{max}$	$-P_{max}$	$+P_{max}$		No		Push down	Pull up
(mm)	(mm)	(mm)	(KN)	(KN)	(N.m)				
$\pm 0\delta_{cy}$	0.00	0.00	0.00	0.00	0.00	0		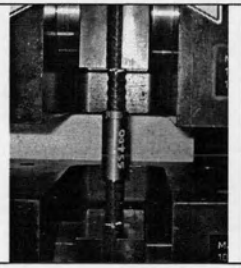	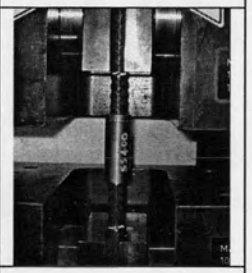
$\pm 3\delta_{cy}$	-1.42	1.14	-165.7	146.4	151.35	1	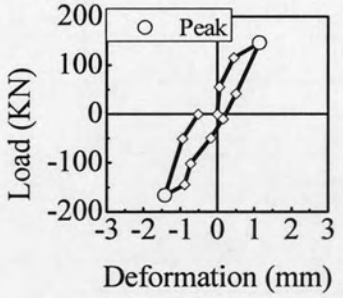		

$\pm 3\delta_{cy}$	-1.36	0.84	-168.4	154.4	180.46	2	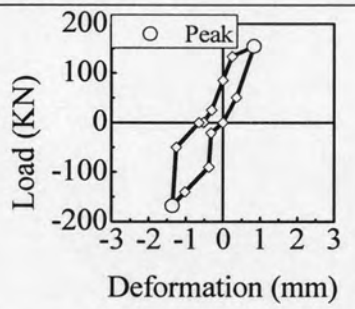	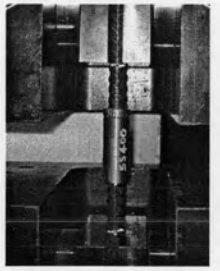	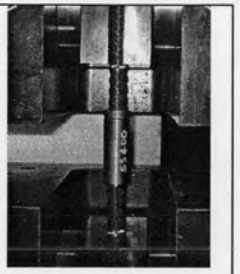
$\pm 6\delta_{cy}$	-2.26	2.06	-168.0	178.9	672.14	3	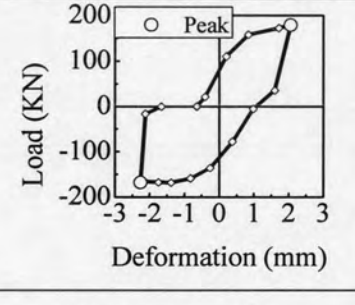	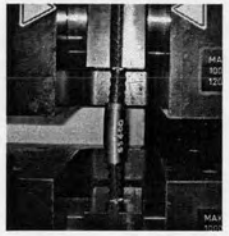	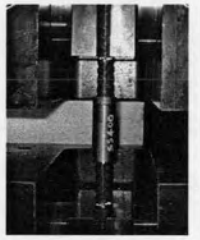
$\pm 6\delta_{cy}$	-2.42	1.98	-155.4	178.3	765.98	4	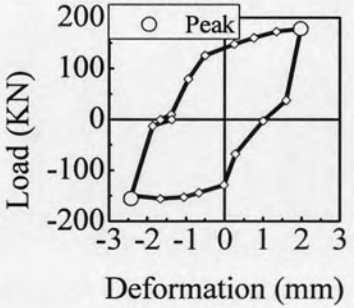	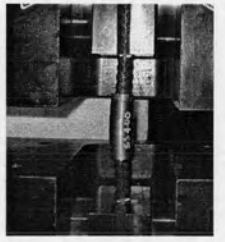	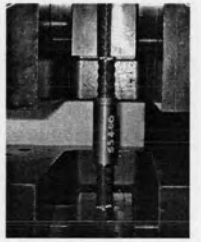

$\pm 9\delta_{cy}$	-1.37	2.98	0	175.0	552.32	5	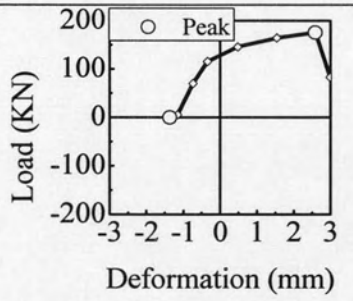	End	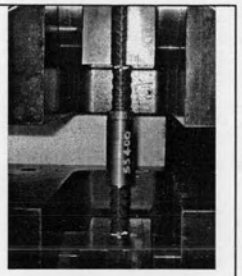

Table B.3 Specimen T4.0-G42 under cyclic loading

Stroke	Deformation		Load		Energy	Cycle	State	Deformed shapes	
	$-\delta_{max}$	$+\delta_{max}$	$-P_{max}$	$+P_{max}$		No		Push down	Pull up
(mm)	(mm)	(mm)	(KN)	(KN)	(N.m)				
$\pm 0\delta_{cy}$	0.00	0.00	0.00	0.00	0.00	0		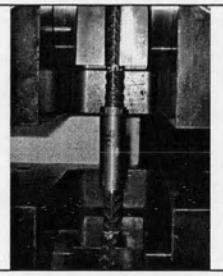	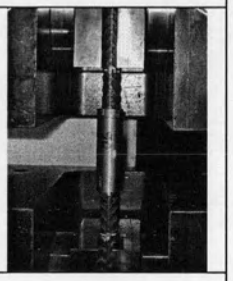
$\pm 3\delta_{cy}$	-1.18	0.98	-163.9	140.5	106.34	1	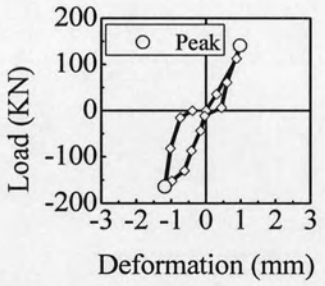		

$\pm 3\delta_{cy}$	-1.22	0.88	-168.3	151.8	100.36	2	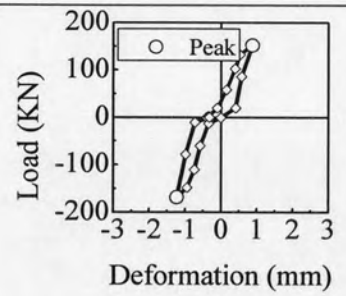		
$\pm 6\delta_{cy}$	-2.12	1.88	-173.3	183.9	533.98	3	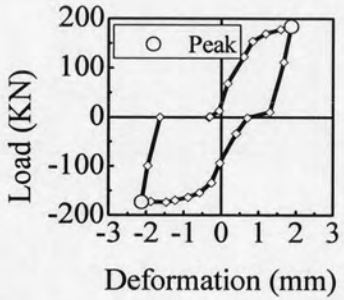	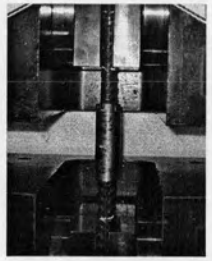	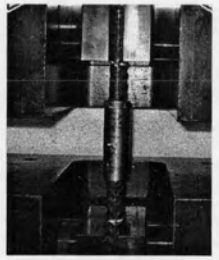
$\pm 6\delta_{cy}$	-2.22	1.74	-163.2	189	583.76	4	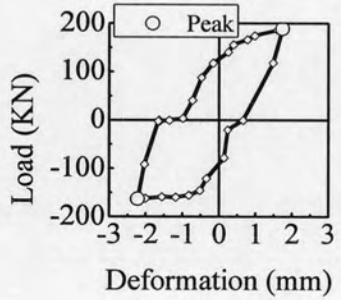	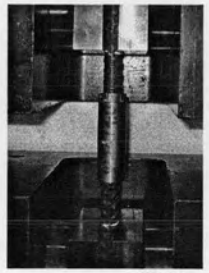	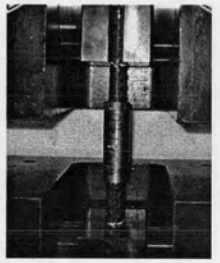

$\pm 9\delta_{cy}$	-3.28	2.72	-158.3	196.20	1078.41	5	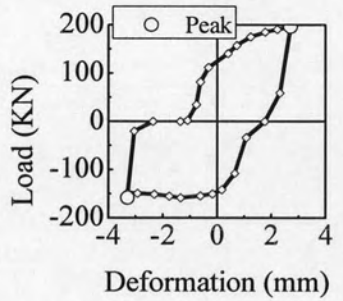	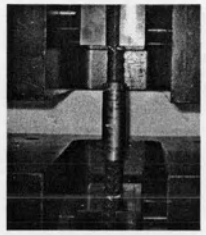	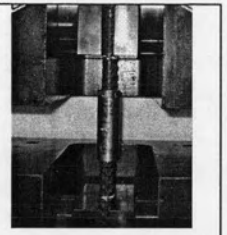
$\pm 9\delta_{cy}$	-2.36	2.02	0	165.8	478.84	6	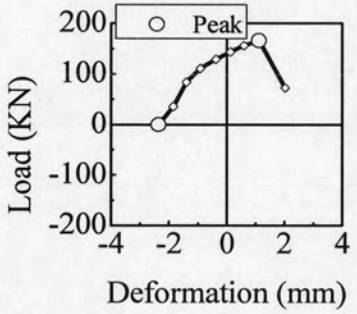	End	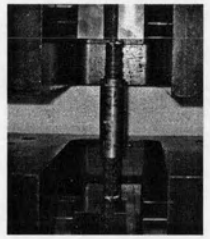

Table B.4 Specimen T4.0-G54 under cyclic loading

Stroke	δ		P		E	Cycle	State	Deformed shapes	
	$-\delta_{max}$	$+\delta_{max}$	$-P_{max}$	$+P_{max}$		No		Push down	Pull up
(mm)	(mm)	(mm)	(KN)	(KN)	(N.m)				
$\pm 0\delta_{cy}$	0.00	0.00	0.00	0.00	0.00	0		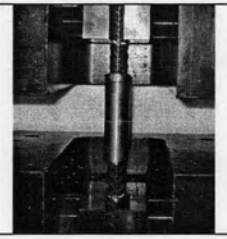	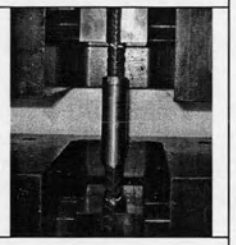
$\pm 3\delta_{cy}$	-1.06	0.90	-165.2	150.24	121.96	1	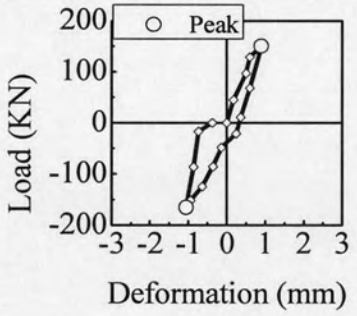		

$\pm 3\delta_{cy}$	-1.44	0.94	-169.9	160.4	126.17	2	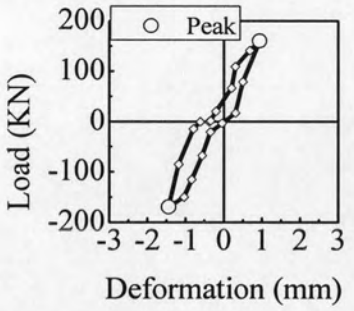		
$\pm 6\delta_{cy}$	-2.26	2.06	-176.3	187.0	650.43	3	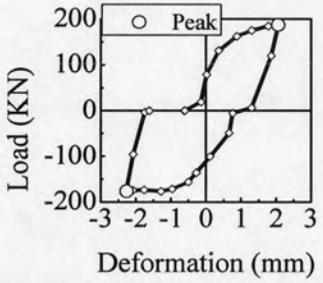		
$\pm 6\delta_{cy}$	-2.04	2.10	-160.3	186	764.07	4	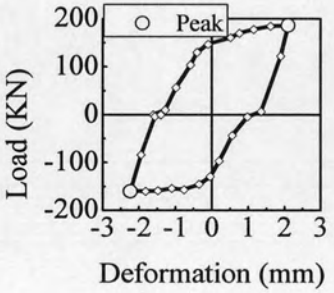	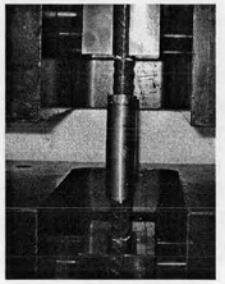	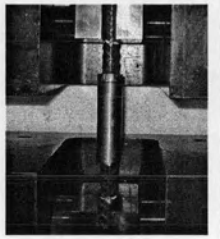

$\pm 9\delta_{cy}$	-2.80	3.74	-149.3	186.0	1318.14	5	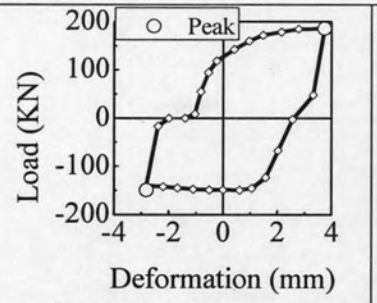	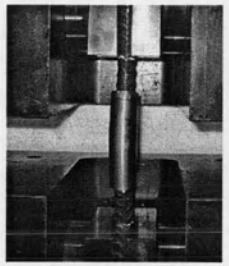	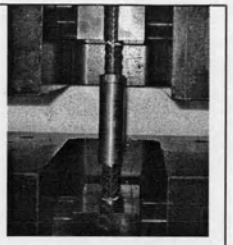
$\pm 9\delta_{cy}$	-1.99	1.82	0	120.2	298.87	6	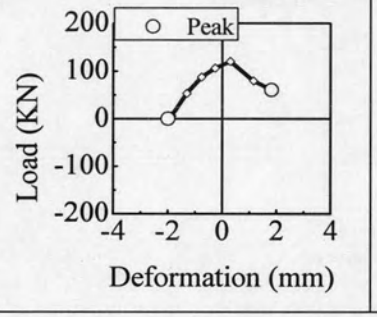	End	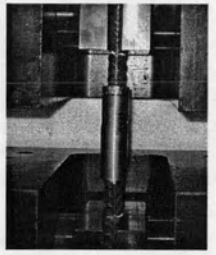

Table B.5 Specimen T4.0-G102 under cyclic loading

Stroke	Deformation		Load		Energy	Cycle	State	Deformed shapes	
	$-\delta_{max}$	$+\delta_{max}$	$-P_{max}$	$+P_{max}$		No		Push down	Pull up
(mm)	(mm)	(mm)	(KN)	(KN)	(N.m)				
$\pm 0\delta_{cy}$	0.00	0.00	0.00	0.00	0.00	0		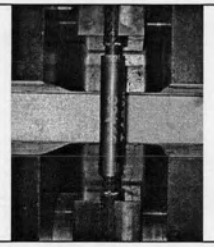	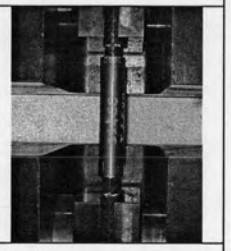
$\pm 3\delta_{cy}$	-1.20	1.02	-151.5	149.4	123.04	1	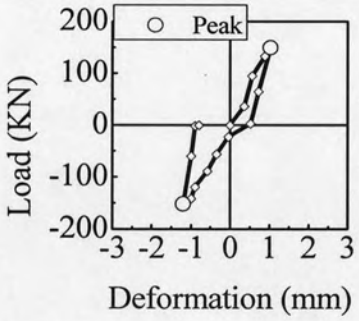	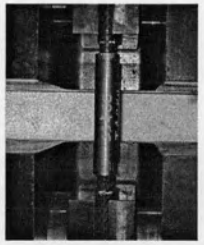	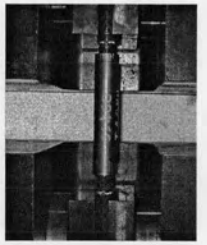

$\pm 3\delta_{cy}$	-1.44	0.96	-151.7	158	209.14	2	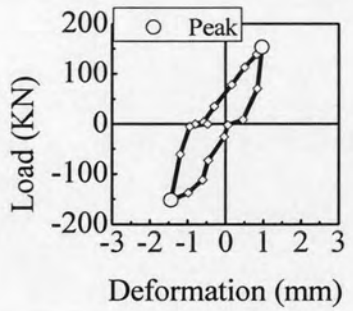	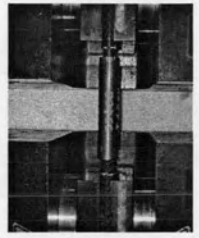	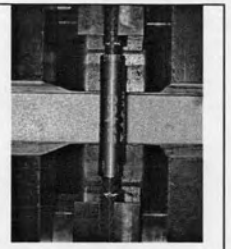
$\pm 6\delta_{cy}$	-3.38	2.46	-179.6	174.5	906.92	3	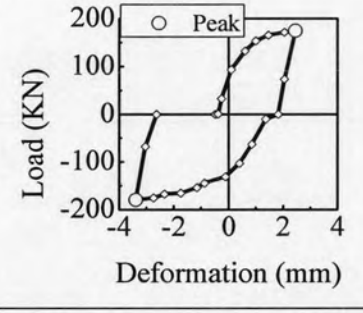	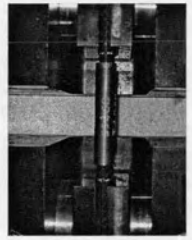	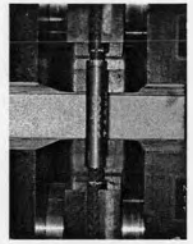
$\pm 6\delta_{cy}$	-3.44	2.30	-176.6	176.3	1192.52	4	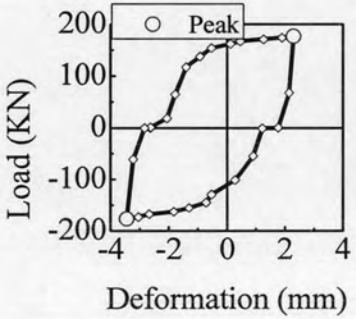	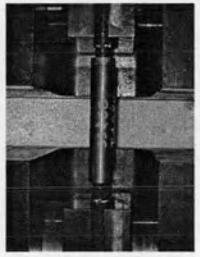	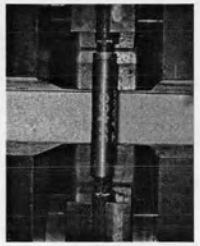

$\pm 9\delta_{cy}$	-5.5	4.02	-176.7	176.3	2100.72	5	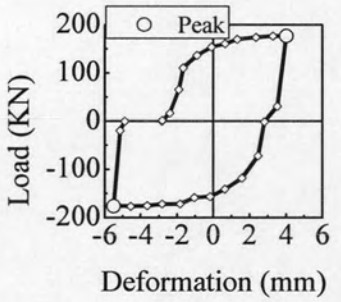	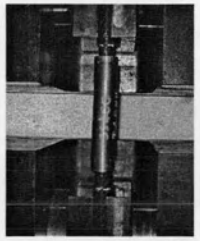	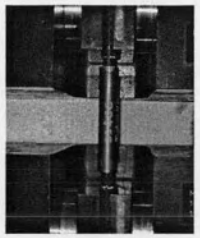
$\pm 9\delta_{cy}$	-4.88	3.92	-146.7	176.5	1487.49	6	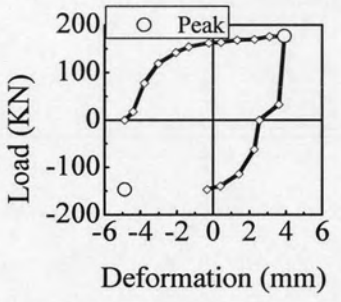	End	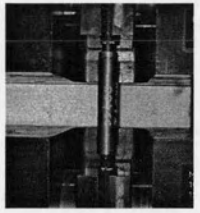

APPENDIX C

C.1 Description of the highway bridge pier

The plan view and elevation view are shown in Figure C.1 and Figure C.2 While Figure C.3 shows the detail of the column and Figure C.4 shows the column sectional properties.

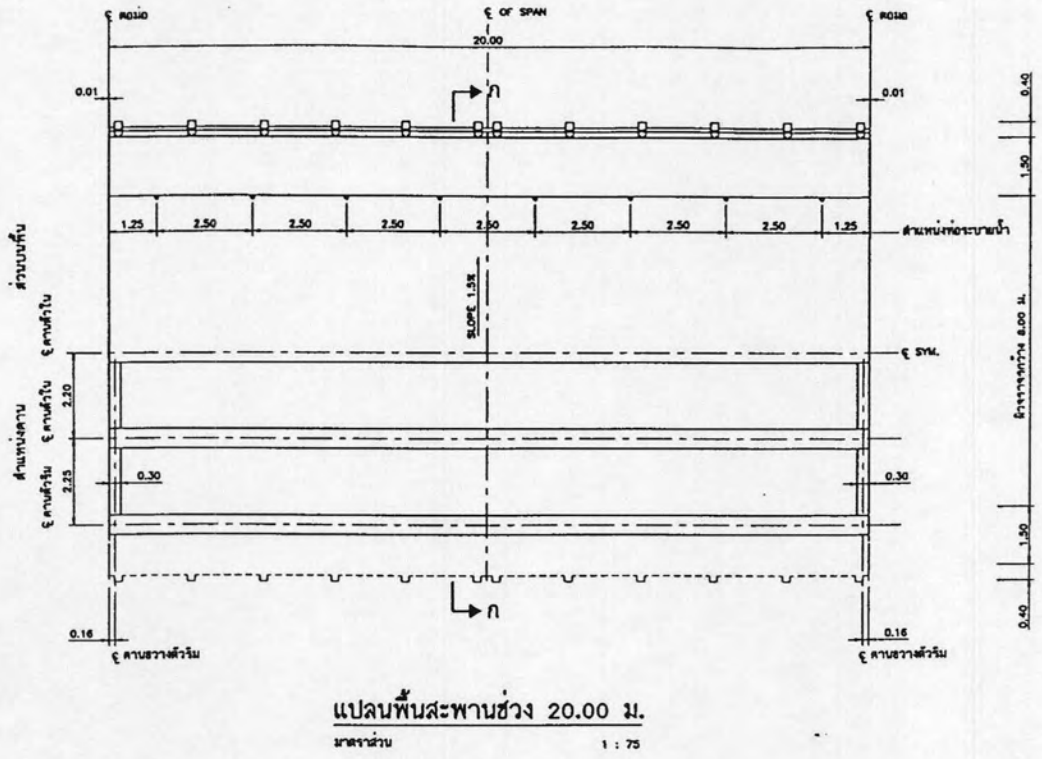

Figure C.1 Plan view of bridge slab for span length of 20m

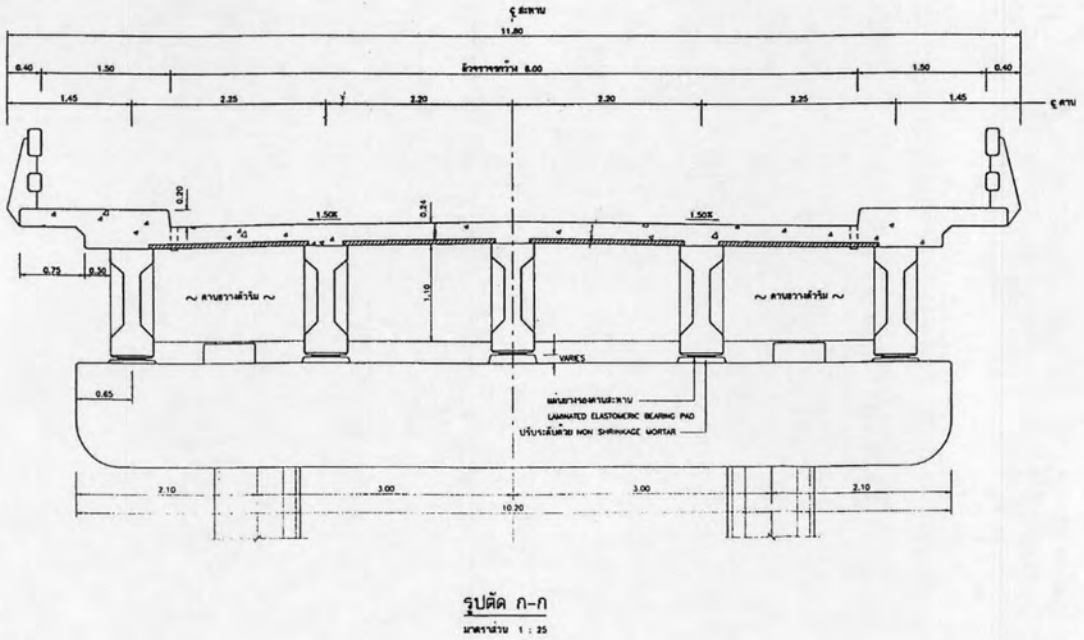

รูปตัด ก-ก
มาตราส่วน 1 : 25

Figure C.2 Elevation of bridge slab for span length of 20m

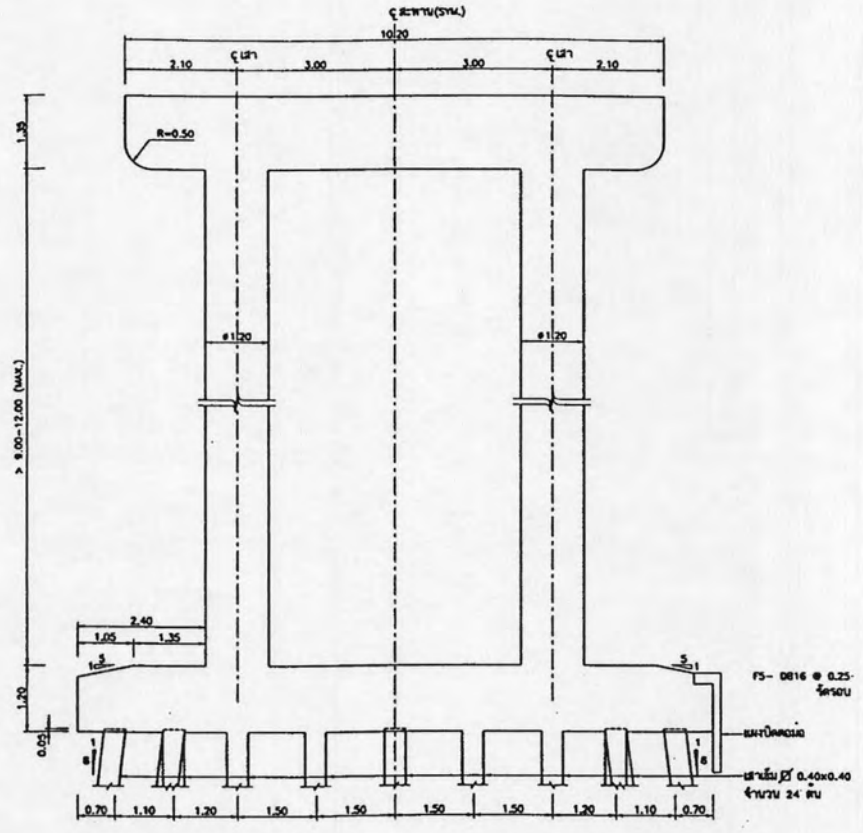

ครึ่งด้านกรณีไม่มีแผงปิดตอม่อ ครึ่งด้านกรณีมีแผงปิดตอม่อ

รูปด้านหน้า
มาตราส่วน 1 : 50

Figure C.3 Front view of bridge piers

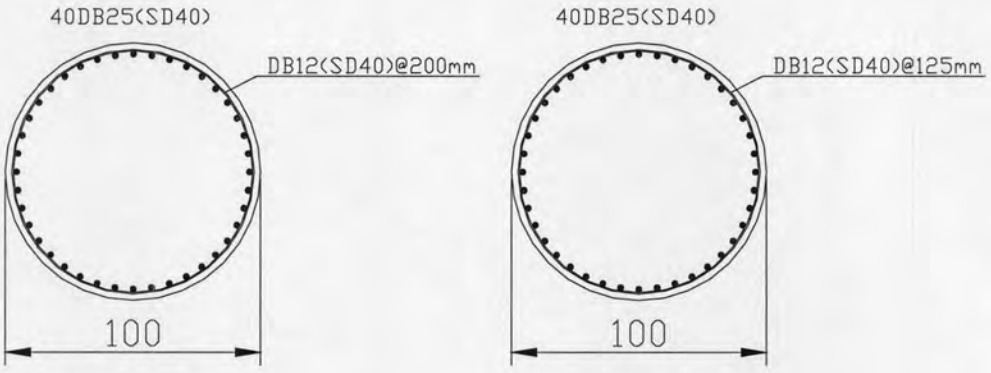

(a). Middle height (b) Bottom height

Figure C.4 Section properties of highway bridge piers

Table C.1 Total section properties of highway bridge column

Section type	Circular	Remark
Column height (m)	6	
Section diameter (m)	1	
Effective depth (m)	0.8	
Gross section area (m2)	0.7854	
Moment of inertia (m4)	0.049088	
Radius of gyration (m)	0.25	
Slenderness ratio	24	
Axial load ratio (Nu/fc'Ag)	0.087	
Concrete cover (m)	0.05	
Concrete strength (MPa)	24.52	
Longitudinal reinforcement ratio (%)	2.50	
Volumetric ratio (%)	0.251 and 0.402	Middle and bottom sections
Maximum moment capacity (MN.m)	3.653	
Shear force (MN)	0.609	
Concrete shear strength (MN)	0.762	
Lateral reinforcement shear strength (MN)	0.568	
Shear ratio	0.154	
Shear force/Shear strength	0.458	Flexural failure mode

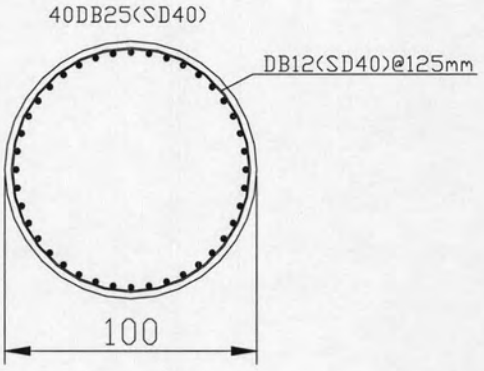

(a) Bottom section

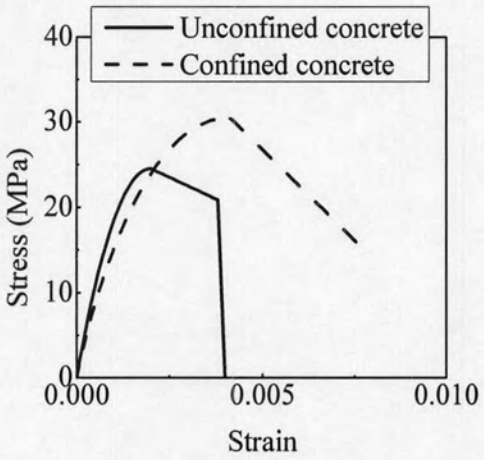

(b) Concrete models

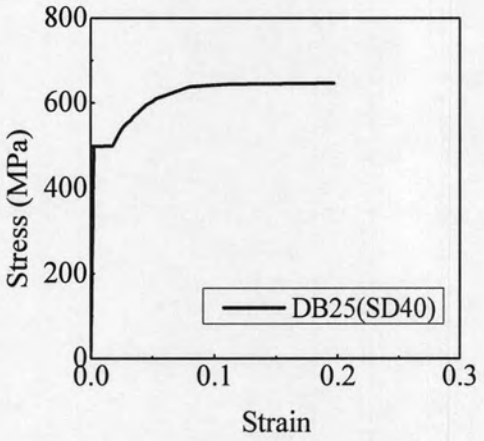

(c) Tensile envelope

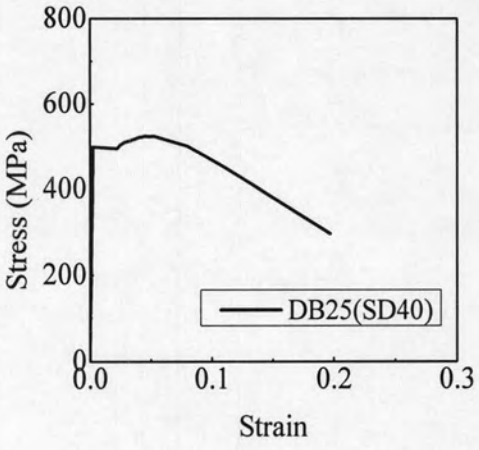

(d) Compressive envelope (Dhakal model)

Figure C..5 Section properties of highway bridge piers

Table C.2: Analysis result at various states of RC section

(Volumetric ratio =0.77%)

States	Material	Strain	Stress	Curvature	Moment
		(10^{-3})	(MPa)	(1/m x10^{-3})	(MN.m x10^{-3})
Crack	Unconfined concrete	o.46	9.95	2.60	81.70
	Confined concrete	0.39	7.48		
	Tensile envelope	0.42	86.37		
	Compressive envelope	0.35	70.96		
Yielding of steel	Unconfined concrete	2.09	23.94	15.8	296.8
	Confined concrete	1.67	22.04		
	Tensile envelope	3.19	557.00		
	Compressive envelope	1.42	290.6		
Cover concrete spalling	Unconfined concrete	4.00	0.00	37.0	313.6
	Confined concrete	3.58	24.13		
	Tensile envelope	7.80	558.60		
	Compressive envelope	3.00	589.5		
Failure	Unconfined concrete	20.81	0.00	127.7	260.5
	Confined concrete	17.40	5.28		
	Tensile envelope	21.89	572.3		
	Compressive envelope	15.40	468.0		

Table C.3: Analysis result at various states of Precast section with mechanical splice T4.0-G54 (Volumetric ratio =0.77%)

States	Material	Strain	Stress	Curvature	Moment
		(10^{-3})	(MPa)	(1/m x10^{-3})	(MN.m x10^{-3})
Crack	Unconfined concrete	0.46	9.87	2.60	76.30
	Confined concrete	0.38	7.41		
	Tensile envelope	0.42	73.13		
	Compressive envelope	0.34	59.61		
Yielding of coupler	Unconfined concrete	1.97	24.50	15.8	256.6
	Confined concrete	1.57	21.33		
	Tensile envelope	3.30	446.90		
	Compressive envelope	1.30	225.70		
Cover concrete spalling	Unconfined concrete	4.00	0.00	47.0	299.0
	Confined concrete	5.012	18.70		
	Tensile envelope	9.45	569.4		
	Compressive envelope	4.28	495.3		
Failure	Unconfined concrete	73.61	0.00	316.8	235.3
	Confined concrete	65.69	5.28		
	Tensile envelope	32.29	627.20		
	Compressive envelope	60.20	423.80		

APPENDIX D

Program for calculation of lateral force-displacement relation of column

D.1 Main program (MatLab)

```
% ********************************************************************
%Program for analysis of load-displacement analysis of column
%Written by Phonepheth Mounnarath on 27/02/2007 and updated on
04/04/2007
% ********************************************************************

clear;
clc;
close all;

%1.IMPORT Data from Moment-Curvature analysis and difinite data
%Curvature(1/m);Moment(MN.m)
%1.1 Data fo column 400mm (Dc=97.5, s=100mm)
%1.1.1 Import data from m-files

mq1 =
textread('mq_c400_S100_01.m','','commentstyle','matlab','delimiter','
');
mq2 =
textread('mq_c400_S100_02.m','','commentstyle','matlab','delimiter',''
);

mq13 =
textread('mq_c400_S100_t40_13.m','','commentstyle','matlab','delimite
r',' ');    %Lowest section 1
mq23 =
textread('mq_c400_S100_t40_23.m','','commentstyle','matlab','delimite
r',' ');    %Lowest section 2

%1.1.2 Difinite the data

c_11=mq1(:,1);   %Curvature of section at top zone (from zero to peak
value)
m_11=mq1(:,2);   %Moment of section at top zone (from zero to peak
value)

c_12=mq1(:,1);  %Curvature of section at middle hieght (from zero to
peak value)
m_12=mq1(:,2);  %Moment of section at middle hieght (from zero to
peak value)

c_13=mq13(:,1);  %Curvature of section at confinement zone (from zero
to peak value)
m_13=mq13(:,2);  %Moment of section at confinement zone (from zero to
peak value)
```

```
c_2=mq23(:,1);   %Curvature of section at confinement zone (from peak
to ultimate)
m_2=mq23(:,2);   %Moment of section at confinement zone (from peak to
ultimate)

h_c=3.0     ; %m Column height

% 1.2 Interpolation of curvatures from the moments
% 1.2.1 Identify the order of moment and devide each moment by column
hieght.
% A.Devide the column height to have 601 sections

    No_use0=length(mq13);    %Number of data point of mq1
    k_0=0;
    for j_0=1:No_use0;
        j_0;
        p_k=m_13(j_0,1)/h_c;

%A1.Part 1 h=0-2.5m;

        i_0=1;
        for y_1=0:0.005:2.5;
            m_i1=p_k*y_1;
            h_1=y_1;
            mo_1=m_i1;
            s_1(i_0,1)=h_1;
            s_1(i_0,2)=mo_1;
        i_0=i_0+1;
        end
        s_1;
        m_k1=s_1(:,2);
        c_k1 = interp1(m_11,c_11,m_k1,'cubic');

%A2.Part 2 h=2.505-2.8m;

        i_0=1;
        for y_2=2.505:0.005:2.8;
            m_i2=p_k*y_2;
            h_2=y_2;
            mo_2=m_i2;
            s_2(i_0,1)=h_2;
            s_2(i_0,2)=mo_2;
        i_0=i_0+1;
        end
        s_2;
        m_k2=s_2(:,2);
        c_k2 = interp1(m_12,c_12,m_k2,'cubic');

%A3.Part 3 h=2.805-3.0m;

        i_0=1;
        for y_3=2.805:0.005:3.0;
            m_i3=p_k*y_3;
            h_3=y_3;
            mo_3=m_i3;
            s_3(i_0,1)=h_3;
            s_3(i_0,2)=mo_3;
        i_0=i_0+1;
```

```
        end
        s_3;
        m_k3=s_3(:,2);
        c_k3= interp1(m_13,c_13,m_k3,'cubic');

%1.2.2  Combination of matrixs to be Total Moment abd curvature

        m_k=[m_k1;m_k2;m_k3];
        c_k=[c_k1;c_k2;c_k3];

%2.Calculate the dispacements and load from the curvatures and
moments
%2.1 Intergration of curvature at the elastic range

        y_a=0:0.005:3.0;
        z1=y_a;
        y_i1=z1';
        No_c_k=size(c_k);
        No_int1=No_c_k(1,1);  % No of points for integration
        No_use1=No_int1-1;
        w=0;
        while w<No_int1
        w=w+1;
        end
        y_i1;
        i_1=1;
        for j_1=1:1:No_use1;
            j_1;

d_1=1/2*(c_k(j_1,1)*y_i1(j_1,1)+c_k(j_1+1,1)*y_i1(j_1+1,1))*(y_i1(j_1
+1,1)-y_i1(j_1,1));
            disp_1=d_1;
            s_a1(i_1,1)=j_1;
            s_a1(i_1,2)=disp_1;
            i_1=i_1+1;
        end
        s_a1;
        d_i1=sum(s_a1(:,2));
    k_0=k_0+1;
    p_n=p_k;
    d_n=d_i1;
    pd_t(k_0,1)=p_n;
    pd_t(k_0,2)=d_n;
    end
    pd_t;
    p1=pd_t(:,1);
    disp1=pd_t(:,2);

%2.2 Calculate the displacements and loads after the peak load

    No_use13=length(mq13);
    disp_y=pd_t(No_use13,2); ; %m  (displacement at peak load)
    c_y=mq13(No_use13,1);      %1/m (Curvature at peak load)
    l_p=0.20;                  %m (plastic hinge length)

    No_use2=length(mq23) ;
    i_2=1;
        for j_2=1:1:No_use2;
```

```
            j_2;
            d_2=disp_y+(c_2(j_2,1)- c_y)*l_p*(h_c-l_p/2);
            p_2=m_2(j_2,1)/h_c;
            disp_2=d_2;
            s_a2(i_2,1)=p_2;
            s_a2(i_2,2)=disp_2;
            i_2=i_2+1;
        end
        s_a2;
        p2=s_a2(:,1);
        disp2=s_a2(:,2);

% 3.Plot the moment-curvature and load-displacement diagram

    figure(1);
    plot(c_11,m_11,'k-','linewidth',1.5)
    xlabel('Curvature(1/m.E-3)');
    ylabel('Moment(MN.m.E-3)');
    grid on;
    figure(2);
    plot(disp1,p1,'m','linewidth',1.5)
    xlabel('Displacement(m.E-3)');
    ylabel('Load(MN.E-3)');
    grid on;

    figure(3);
    plot(c_2,m_2,'k-','linewidth',1.5)
    xlabel('Curvature(1/m.E-3)');
    ylabel('Moment(MN.m.E-3)');
    grid on;

    figure(4);
    plot(disp2,p2,'m','linewidth',1.5)
    xlabel('Displacement(m.E-3)');
    ylabel('Load(MN.E-3)');
    grid on;

    figure(5);
    plot(c_13,m_13,'k-','linewidth',1.5)
    hold on;
    plot(c_2,m_2,'m--','linewidth',1.5)
    xlabel('Curvature(1/m.E-3)');
    ylabel('Moment(MN.m.E-3)');
    grid on;

    figure(6);
    plot(disp1,p1,'k-','linewidth',1.5)
    hold on;
    plot(disp2,p2,'m--','linewidth',1.5)
    xlabel('Displacement(m.E-3)');
    ylabel('Load(MN.E-3)');
    grid on;

%4.Exporting the data to be m-files and Excel files
%4.1 Prepare the data by making rows
%A. Data for exporting to m-files
%A.1 The lateral displacements and loads (from zero to peak value)
```

```
a=[disp1 p1];
w=a';

%A.2 The lateral displacements and loads (from peak to final value)

b=[disp2 p2];
g=b';

%B. Data for exporting to Excel-files
%B.1 The lateral displacements and loads (from zero to peak value)

c=[disp1 p1];
y=c';

%B.2 The lateral displacements and loads (from peak to final value)

d=[disp2 p2];
z=d';

%4.2 Exporting data to m-files(file name.m) and Excel-files(file
name.dat)

out_put1=w;
out_put2=g;
out_put3=y;
out_put4=z;

file_out1=fopen('pd1.m','w');
file_out2=fopen('pd2.m','w');
file_out3=fopen('dp1.dat','w');
file_out4=fopen('dp2.dat','w');

fprintf(file_out1,'%6.6f %12.8f\n',out_put1);
fprintf(file_out2,'%6.6f %12.8f\n',out_put2);
fprintf(file_out3,'%6.6f %12.8f\n',out_put3);
fprintf(file_out4,'%6.6f %12.8f\n',out_put4);

fclose(file_out1);
fclose(file_out2);
fclose(file_out3);
fclose(file_out4);

%End of the program
```

APPENDIX E

E.1 Load and voltage calibration of actuator Instron

First test		Second test		Third test		Average value	
Load	Voltage	Load	Voltage	Load	Voltage	Load	Voltage
(KN)	(v)	(KN)	(v)	(KN)	(v)	(KN)	(v)
10	0.1005	10	0.1005	10	0.1005	10	0.101
20	0.2005	20	0.2005	20	0.2005	20	0.201
30	0.3005	30	0.3005	30	0.3005	30	0.301
40	0.3980	40	0.3990	40	0.3990	40	0.399
50	0.4980	50	0.4980	50	0.4980	50	0.498
60	0.5980	60	0.5980	60	0.5980	60	0.598
70	0.6980	70	0.6980	70	0.6980	70	0.698
80	0.7980	80	0.7970	80	0.7980	80	0.798
90	0.8970	90	0.8970	90	0.8970	90	0.897
100	0.9970	100	0.9970	100	0.9970	100	0.997

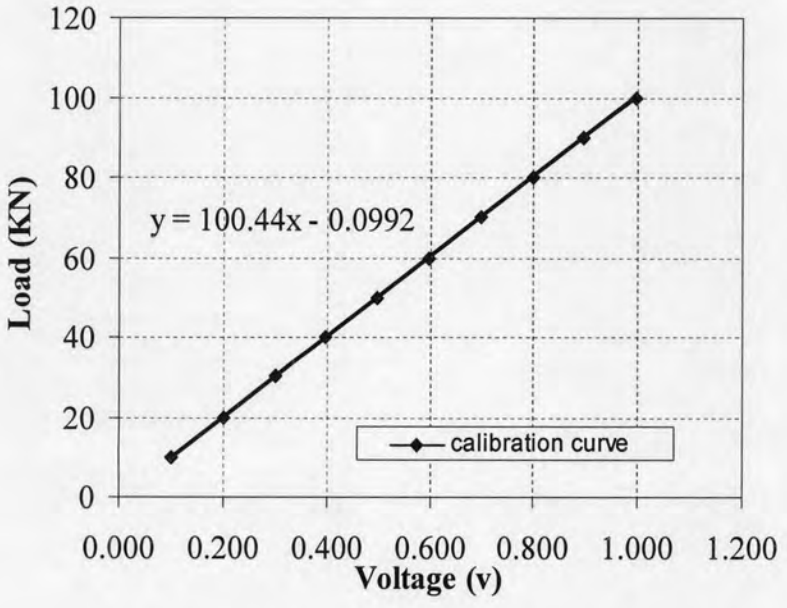

Figure E.1 Calibration of load and voltag

E.2 Stroke and voltage calibration of actuator Instron

First test				Second test				Average Value			
Position	Voltage	Position	Voltage	Position	Voltage	Position	Voltage	Position	Voltage	Position	Voltage
(mm)	(v)	(mm)	(v)	(mm)	(v)	(mm)	(v)	(mm)	(v)	(mm)	(v)
0	0.003	0	0.003	0	0.003	0	0.003	0	0.003	0	0.003
10	0.799	-10	-0.794	10	0.799	-10	-0.794	10	0.799	-10	-0.794
20	1.596	-20	-1.591	20	1.596	-20	-1.591	20	1.596	-20	-1.591
30	2.393	-30	-2.388	30	2.393	-30	-2.389	30	2.393	-30	-2.389
40	3.191	-40	-3.186	40	3.191	-40	-3.186	40	3.191	-40	-3.186
50	3.990	-50	-3.990	50	3.990	-50	-3.990	50	3.990	-50	-3.990
60	4.790	-60	-4.790	60	4.790	-60	-4.790	60	4.790	-60	-4.790
70	5.590	-70	-5.590	70	5.590	-70	-5.590	70	5.590	-70	-5.590
80	6.390	-80	-6.390	80	6.390	-80	-6.390	80	6.390	-80	-6.390
90	7.190	-90	-7.190	90	7.190	-90	-7.190	90	7.190	-90	-7.190
100	7.990				7.990			100	7.990		

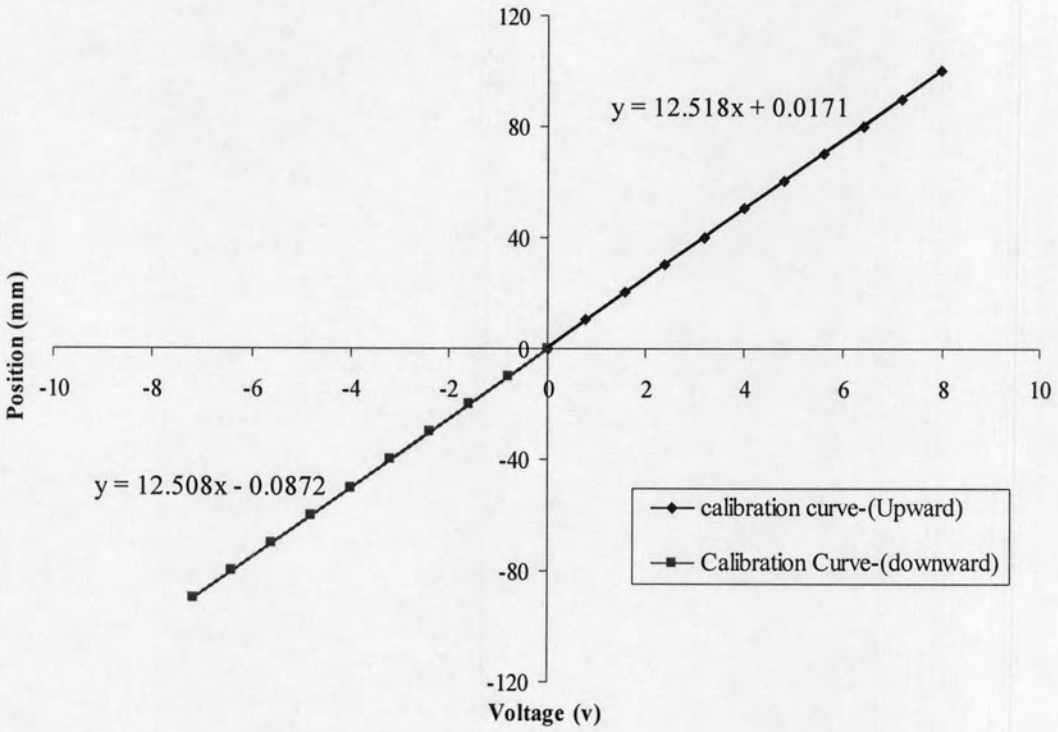

Figure E.2 Calibration of load and voltag

E.2 Voltage and displacement calibration of displacement transducer

Voltgae (v)	Displacement (mm)
1.476	0.1476
1.982	0.1982
2.492	0.2492
3.001	0.3001
3.51	0.351
4.02	0.402
4.67	0.467
5.32	0.532
5.97	0.597
6.62	0.662

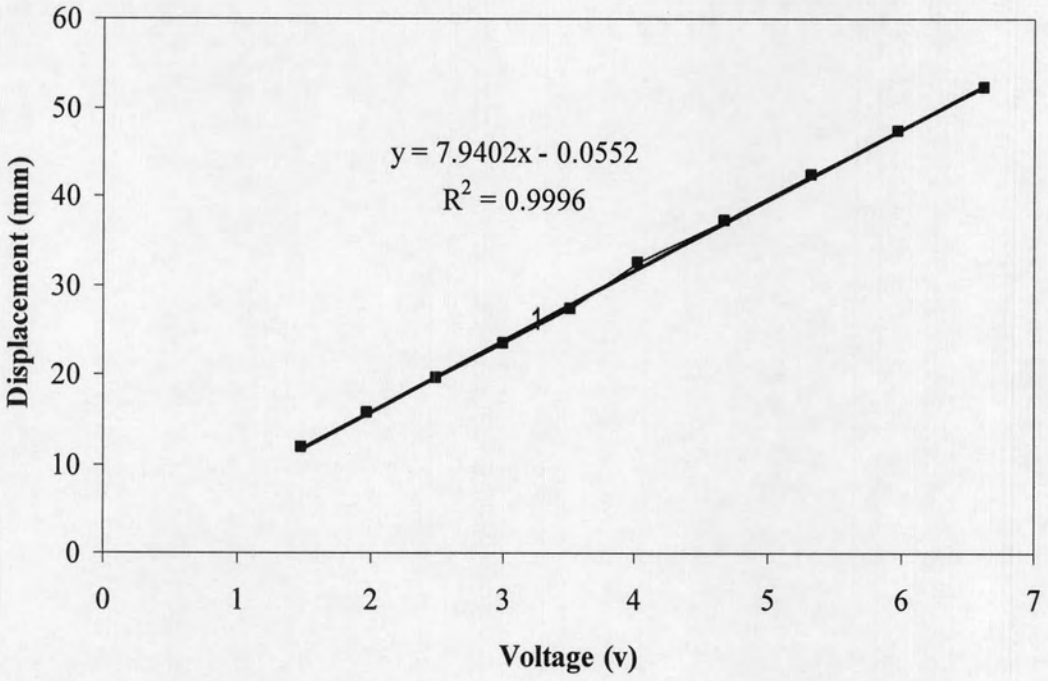

Figure E.3 Calibration of displacement and voltag

BIOGRAPHY

Phonepheth Mounnarath

He was born in Vientiane, the capital city of Laos, on the 8th of December, 1982. He gained his primary and secondary education from schools in Banhom, Pafang Village, Hathxayfong District located near my hometown. From 1999 to 2004, he pursued undergraduate studies in Civil Engineering at the National University of Laos. After graduation, he received the AUN/SEED-Net Scholarship to further his study for Master's degree in Structural Engineering. He conducted this study with the thought that it will be useful for his country in the near future.